

ple is heated from liquid helium to liquid nitrogen temperature (Fig. 7) is a consequence of the growing damping of acoustic waves by lattice vibrations because the lattice temperature rises.

The authors are grateful to L. M. Novak for preparing the samples.

- <sup>1</sup>V. N. Ivanov, M. S. Murashov, and A. P. Shotov, Proc. Eleventh Intern. Conf. on Physics of Semiconductors, Warsaw, 1972, Vol. 1, publ. by PWN, Warsaw (1972), p. 170.
- <sup>2</sup>J. R. Haynes and N. G. Nilsson, Proc. Seventh Intern. Conf. on Physics of Semiconductors, Paris, 1964, Vol. 4, Radiative Recombination in Semiconductors, publ. by Dunod, Paris; Academic Press, New York (1965), p. 21.
- <sup>3</sup>R. J. Elliott, Phys. Rev. **108**, 1384 (1957).
- <sup>4</sup>E. M. Conwell, High Field Transport in Semiconductors, Suppl. 9 to Solid State Phys., Academic Press, New York, 1967, (Russ. Transl., Mir, M., 1970).
- <sup>5</sup>A. K. Pustovoit, Fiz. Tekh. Poluprovodn. **5**, 1989 (1971) [Sov. Phys. Semicond. **5**, 1725 (1972)].
- <sup>6</sup>G. Weinreich, T. M. Sanders Jr, and H. G. White, Phys. Rev. **114**, 33 (1959).
- <sup>7</sup>M. A. Isakovich, Obshchaya akustika (General Acoustics), Nauka, M., 1973.
- <sup>8</sup>V. L. Gurevich and B. D. Laikhtman, Fiz. Tverd. Tela (Leningrad) **7**, 3218 (1965) [Sov. Phys. Solid State **7**, 2603 (1966)].
- <sup>9</sup>J. D. Maines and E. G. S. Paige, J. Phys. C **2**, 175 (1969).
- <sup>10</sup>R. A. Heising (ed.), Quartz Crystals for Electrical Circuits, Van Nostrand, New York, 1946.
- <sup>11</sup>J. W. S. Rayleigh, The Theory of Sound, 2nd ed., 2 Vols., MacMillan, London, 1894-6, reprinted by Dover, New York, 1945 (Russ. Transl., Gostekhizdat, M., 1945).
- <sup>12</sup>L. É. Gurevich and T. M. Gasymov, Fiz. Tverd. Tela (Leningrad) **9**, 106 (1967) [Sov. Phys. Solid State **9**, 78 (1967)].
- <sup>13</sup>V. L. Gurevich and B. D. Laikhtman, Zh. Eksp. Teor. Fiz. **46**, 598 (1964) [Sov. Phys. JETP **19**, 407 (1964)].

Translated by A. Tybulewicz

## Determination of the density of phonon states of naphthalene crystal from inelastic incoherent neutron scattering

É. L. Bokhenkov, I. Natkaniec,<sup>1)</sup> and E. F. Sheka

*Institute of Solid State Physics, USSR Academy of Sciences*  
(Submitted July 30, 1975; resubmitted November 5, 1975)  
Zh. Eksp. Teor. Fiz. **70**, 1027-1043 (March 1976)

The spectra of the inelastic incoherent neutron scattering from a naphthalene crystal were obtained at temperatures 4.7, 80, and 296°K in the energy-transfer region 0-1300 cm<sup>-1</sup>. The direct and inverse spectral problems are analyzed as mathematical methods for obtaining from experimental spectra information on the density of the phonon states of the crystal. The fundamental difficulties of the method of the inverse spectral problem are discussed. It is shown that no consistent application of this method is possible without an independent solution of the model dynamic problem of the crystal. Under these conditions, the use of the direct spectral problem is more productive. A solution of the direct spectral problem is obtained for the naphthalene crystal. The density of the phonon states of the crystal in the energy range 0-1300 cm<sup>-1</sup> is determined by comparing the experimental results with the calculations.

PACS numbers: 61.12.Fy, 63.20.Dj

### INTRODUCTION

It is widely known that inelastic scattering of slow neutrons in a crystal can serve as the most direct method of studying its phonon spectrum.<sup>[1-5]</sup> Neutron spectroscopy of phonons, however, which is a realization of this possibility, has not yet become as widely used a method for the studying of the phonon spectrum as, for example, optical spectroscopy. This is caused not only by the complexity of the neutron-spectroscopy experiment and the need for operating with beams of slow neutrons of sufficient density. Greater difficulties are encountered when it comes to extracting information on the phonon spectrum of crystal from the experimental neutron-scattering spectrum. This pertains first of all to the determination of the density of states of the phonon spectra. This question was raised in the literature many times (see<sup>[2,3,6-8]</sup>), but until recently only the connection between the neutron scattering cross section

and the density of the phonon states was considered. It was assumed there that the inelastic scattering cross section (and moreover single-phonon scattering) is obtained from the experimental results. Actually, the determination of the scattering cross section from the experimentally measured spectrum is a rather difficult mathematical problem, so that means of obtaining its solutions must be considered. We shall discuss this problem below for the case of incoherent inelastic scattering. The main conclusions will be illustrated with an analysis of the spectra of neutron scattering in a naphthalene crystal, and a connection will be established between these spectra and the density of the phonon states of the crystal.

### 1. DIRECT AND INVERSE SPECTRAL PROBLEMS IN NEUTRON-SCATTERING SPECTROSCOPY

In the experimental method of measuring the energy of the scattered neutrons by their time of flight, a

scattering spectrum for the incoherent inelastic neutron scattering (IINS) is (see, e.g., [9])

$$N(t_0) = \Delta t_0 \iiint dE_0 dE dt F(E_0, E, t_0, t) \sigma(E_0, E, \varphi, T), \quad (1)$$

$$F(E_0, E, t_0, t) = A(E_0, E, t_0, t) \rho(E_0, t) n(E_0) \Phi(E), \quad (1a)$$

where  $N(t_0)$  is the number of neutrons arriving from the analyzer within the time interval  $\Delta t_0$  by the instant of time  $t_0$ ,  $\sigma(E_0, E, \varphi, T)$  describes the law of scattering by the nuclei ( $E_0$  and  $E$  are the energies of the incident and registered neutrons,  $\varphi$  is the scattering angle, and  $T$  is the temperature),  $F(E_0, E, t_0, t)$  is the apparatus function of the instrument and constitutes the kernel of the convolution in the integral equation (1). The functions describing  $F$  in (1a) correspond to the temporal ( $\rho(E_0, t)$ ) and energy ( $n(E_0)$  and  $\Phi(E)$ ) distributions of the incident and registered neutrons, while  $A(E_0, E, t_0, t)$  takes into account the additional specific features of the dispersing and analyzing devices of the employed neutron spectrometer.<sup>[2]</sup>

As seen from (1), the measured function  $N(t_0)$  and the sought function  $\sigma(E_0, E, \varphi, T)$  can differ from each other even qualitatively. The establishment of the quantitative connection between  $N$  and  $\sigma$  is the gist of the mathematical reduction common to many spectral problems.

There are two variants of solving this problem: the variant of the inverse spectral problem, when the functions  $N$  and  $F$  are assumed given, and the variant of the direct spectral problem, when the functions  $F$  and  $\sigma$  are given.

#### A. The inverse spectral problem

This variant seems preferable, since it does not call for simulating the dynamic problem of the crystal. Its subsequent realization, however, encounters serious difficulties. The first difficulty is connected with the very solution of the inverse-convolution problem, which was recently analyzed in detail in [10, 11]. On the other hand, if this problem is solved and the function  $\sigma$  is obtained sufficiently reliably, then a second problem arises, because  $\sigma$  is connected sufficiently simply with the phonon spectrum of the crystal only for single-phonon incoherent scattering<sup>[1, 2]</sup>

$$\sigma_i^{\text{inc}}(E_0, E, \varphi, T) = \sum_i \frac{d^2 \sigma_i^{\text{inc}}}{d\omega d\Omega} = \frac{k}{k_0} \frac{\hbar |Q|^2}{2M\omega} \sum_i (b_i^{\text{inc}})^2 \frac{\exp(-2W_i)}{1 - \exp(-\hbar\omega/kT)} G_i^{\text{inc}}(\omega), \quad (2)$$

$$G_i^{\text{inc}}(\omega) = \frac{M}{M_i} \sum_j \int d\mathbf{q} |A_j^i(\mathbf{q})|^2 \delta(\omega - \omega_j(\mathbf{q})), \quad (3)$$

where  $G_i^{\text{inc}}(\omega)$  is the density of the phonon states of the crystal, weighted on the amplitudes of the displacement of the  $i$ -th atom,<sup>[12]</sup> and the remaining notation is standard.<sup>[1, 2, 5]</sup> As to processes with participation of more than one phonon, a correct description of their contribution to the measured scattering spectrum calls for a preliminary solution of the dynamic problem of the crystal.<sup>[5]</sup>

Cases can occur when the single-phonon processes predominate (the region of low temperatures and low

energy transfer to the neutrons). Even in such cases, however, as seen from (2) and (3), for crystals with low symmetry and complicated structures of the unit cell (this is precisely the situation realized for molecular crystals) we can obtain from the experimental spectrum only a generalized description of the photon spectrum, containing both its distribution function and the displacement vectors of the individual atoms. A separate determination of these characteristics calls for a dynamic theoretical calculation. The experimental problem of determining the polarization vectors in a number of reciprocal-lattice points large enough for the calculation ( $\sim 10^4$ ), which is an experimental problem that is feasible in principle, can not be considered seriously as yet.

In practice, in all the known cases where  $g(\omega)$  is determined, the reduction procedure is only a partial solution of the inverse problem. Usually, without an exact solution of the inverse spectral problem for the integral equation (1), a correction is introduced in the measured spectrum  $N(t_0)$  for the background and for a multiple and multiphonon scattering using the general properties of the scattering cross section for these cases.<sup>[6, 7, 13]</sup> Formula (2) is used to eliminate the energy dependences of the incident and registered neutrons, of the angle, and of the temperature, and the curve obtained after such a reduction is usually represented as the experimentally obtained phonon-state density function. Actually, this function turns out to be related to the concrete experimental setup, and its deviation from the true density of states was recently strikingly demonstrated with the phonon spectrum of magnesium as an example.<sup>[14]</sup>

The dependence of the spectral distribution of the IINS and the apparatus function of the spectrometer is shown in Fig. 1. The IINS spectra shown in the figure were obtained for a naphthalene crystal at  $T = 4.7^\circ\text{K}$  with two different time-of-flight spectrometers: the KDSOG-1 inverse-geometry spectrometer with the IBR-1 reactor in Dubna (present work) and the IN4 direct-geometry spectrometer of ILL in Grenoble.<sup>[15]</sup>

It is easily seen that the usually employed procedure, described above, of reducing the experimental spectra leads to essentially different results for one and the same crystal.

#### B. The direct spectral problem

The direct spectral problem is based on a model calculation of the dynamic problem and on the determination, with the aid of this calculation, of the cross section of the single-phonon scattering  $\sigma$  in the form (2). The next step is a convolution of the obtained  $\sigma$  with the apparatus function of the spectrometer  $F(E_0, E, t_0, t)$  and a determination of the "experimental" scattering spectrum obtained in this case in the form (1). A comparison of the calculated and experimental spectra at this level makes possible the following:

1) Determination of the relative role of the multiphonon and the multiple processes in the observed scattering spectrum.

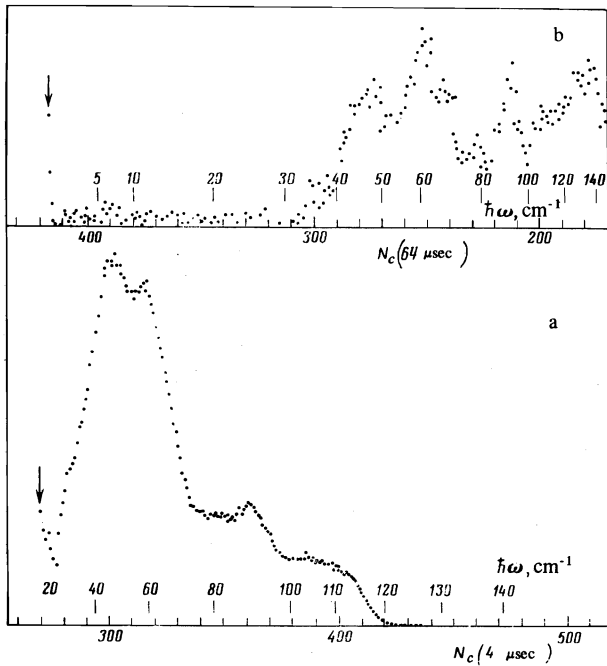


FIG. 1. IINS spectra from a naphthalene crystal in the energy-transfer region  $\hbar\omega \sim 0-130 \text{ cm}^{-1}$ ,  $T=4.7^\circ\text{K}$ : a) direct-geometry spectrometer, <sup>[15]</sup> b) inverse-geometry spectrometer (present work). The arrow shows the position of the elastic peak,  $N_c$  is the channel number.

2) Estimate the applicability of the employed dynamic model in the case when the single-phonon processes predominate, and use the difference between the experimental and calculated spectra to improve the method of solving the dynamic problem and to obtain reliable characteristics of the phonon spectrum of the crystal.

3) Optimize the organization of the expensive present-day experimental scattering spectroscopy.

At present there are only two known applications of the direct spectral problem for the reduction of data on inelastic neutron scattering: for incoherent scattering in a benzene crystal <sup>[16]</sup> and coherent scattering in magnesium. <sup>[14]</sup> We consider this method as applied to IINS in a naphthalene crystal. In contrast to the benzene crystal, <sup>[16]</sup> the experiment on which was performed with insufficient resolution, the good resolution of the experimental scattering spectra of naphthalene made it possible to compare in detail the measured and calculated spectra in accordance with the scheme described above.

## 2. EXPERIMENTAL SPECTRA OF NEUTRON SCATTERING BY A NAPHTHALENE CRYSTAL

The naphthalene crystal, alongside benzene and anthracene, was for many years the main object used to test and develop methods for quantitative investigations of various physical properties of complicated molecular crystals. The phenomenological universality of the intermolecular interaction made it possible to extend these methods to a large class of compounds. This is precisely why the naphthalene crystal was chosen by us to describe the capabilities of the IINS spectroscopy in

quantitative investigations of the phonon-state spectrum.

The IINS spectra from the naphthalene crystal were obtained at temperatures 4.7, 80, and 296 °K by the time of flight method with the KDSOG-1 inverse-geometry spectrometer <sup>[17]</sup> (IBR-1 reactor <sup>[18]</sup>) in the neutron physics laboratory of the Joint Institute for Nuclear Research.

The sample was a finely-dispersed polycrystalline powder (average particle dimension  $\sim 100 \mu$ ) of chromatographically pure naphthalene, filling a cylindrical cell with base diameter 200 mm and height 0.5 mm for the measurements at 80 and 296 °K, and a cell with rectangular 120×50 mm cross section of the same thickness for the measurements at 4.7 °K. The measurement times were 100, 108, and 149 hr respectively for the temperatures 296, 80, and 4.7 °K. The neutron transmission in all cases was  $\sim 85\%$ . The obtained spectra are shown in Fig. 2. The spectra were corrected for the constant background due to the fast neutrons and the cryostat background, summed over five measurement angles (50, 70, 110, 130, and 150 degrees), and reduced to a single effective sample and a single measurement time.

To reduce the experimental data we had to determine the apparatus function of the instrument in the form (1a). The general character of this function was analyzed earlier. <sup>[19]</sup> The functions contained in (1a) are of the form

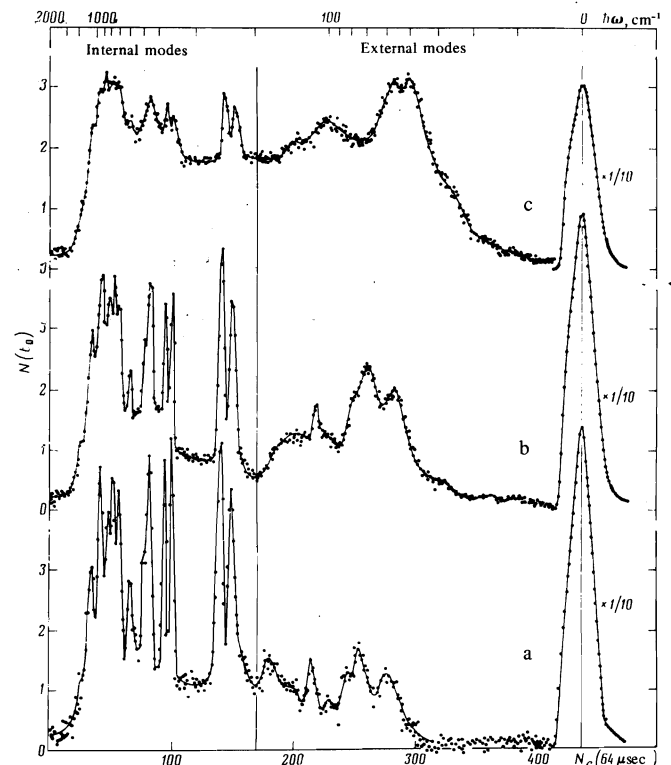


FIG. 2. IINS spectra from a naphthalene crystal in the energy-transfer region  $\hbar\omega \sim 0-1300 \text{ cm}^{-1}$ : a)  $T=4.7^\circ\text{K}$ , b)  $T=80^\circ\text{K}$ , c)  $T=296^\circ\text{K}$ ;  $N(t_0)$  is the normalized scattering intensity and  $N_c$  is the channel number.

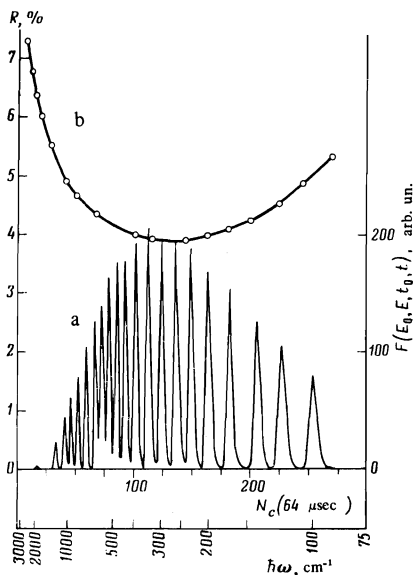


FIG. 3. a) Apparatus function  $F(E_0, E, t_0, t)$  of the inverse-geometry spectrometer KDSOG-1 on the IBR-1 reactor, b) Relative energy resolution function  $R(\omega)$ .

$$n(E_0) = E_0 \exp(-E_0/226)$$

( $E_0$  is in  $\text{cm}^{-1}$ ), corresponding to a Maxwellian neutron distribution in the moderator, with a temperature  $326^\circ\text{K}$ . The approximation by a Maxwellian spectrum accounts well for the spectral distribution of the incident neutrons, as measured experimentally on vanadium, in the given range of energy transfer. The temporal distribution of the incident neutrons was

$$\rho(t, E_0) = \begin{cases} 0, & t < 0 \\ 1 - \exp(-t/\tau), & 0 \leq t \leq t_m \\ [1 - \exp(-t_m/\tau)] \exp(t_m - t/\tau), & t > t_m \end{cases}$$

where<sup>3)</sup> the rise time of the reactor pulse was  $t_m = 130 \mu\text{sec}$ , the lifetime of the neutrons in the moderator was  $\tau(E_0) = 160 \exp\{0.0114 E_0\} [\mu\text{sec}]$ . The lengths of the flight bases were  $L_1 = 30.218$  and  $L_2 = 1.425$  meters.

The energy distribution  $\Phi(E)$  of the registered neutrons were shaped with a beryllium filter and zinc single crystal as the monochrometer ( $1.5^\circ$  mosaic) and is well described in the presented series of experiments by the shape of the elastic peak. The apparatus function  $F(E_0, E, T_0, t)$  of the instrument, determined by the functions given above is shown in Fig. 3 for different values of the energies transferred in the inelastic scattering. The relative energy resolution is shown in the upper part of Fig. 3.

### 3. DYNAMIC MODEL OF CRYSTAL

The phonon spectrum of the naphthalene crystal consists of 108 branches (18 atoms  $\times$  2 molecules  $\times$  3 degrees of freedom), of which 96 are genetically connected with 48 intramolecular vibrations of the molecule and 12 branches are due to translational and rotational motion of the molecules as the units. The dynamics of the molecular crystals has by now been developed in

principle sufficiently well to be able to solve fully the problem of the eigenvalues and eigenvectors of the phonon spectrum of a crystal of the naphthalene type.<sup>[20,21]</sup> However, calculations for a large number of points of the Brillouin zone are a serious computational problem. In most cases it is therefore customary to use for complicated molecular crystals a separation of the phonon spectrum into internal and external modes, based on the significant predominance of the forces of the intramolecular interactions over the external ones.<sup>[22]</sup> The dynamic problem for the crystal is then solved separately for the two types of modes. For the internal modes, a rigid-lattice approximation is used (the intermolecular interaction is assumed to be negligibly small or is taken into account within the framework of perturbation theory).<sup>[23]</sup> The density of the phonon states of this part of the spectrum is a set of  $\delta$  functions in accord with the number of the intramolecular modes. The external modes are considered in the rigid-molecule approximation.<sup>[24]</sup>

The experimental criterion for the validity of this analysis is usually the width of the energy gap between the external and internal modes. As seen from Fig. 2, in the naphthalene crystal the gap is  $50 \text{ cm}^{-1}$  wide, so that the two low-frequency branches of the internal modes are close enough to the high-frequency branches of the external ones. Under these conditions, the separation of the dynamic problems into two in accordance with the assumptions made above is not rigorous. However, an analysis of the results of the solution of the complete dynamic problem for naphthalene, obtained for the symmetrical b direction,<sup>[20]</sup> has shown that the values of the resonant splitting of the phonon modes in the center of the Brillouin zone exceed  $10 \text{ cm}^{-1}$  for only three modes in the region of the internal modes. For the remaining modes this value is much less than  $10 \text{ cm}^{-1}$ . At the same time, the frequency shift of the internal phonon modes relative to the vibrations of the free molecule, as seen from the calculation<sup>[20]</sup> and as follows from experiment, also does not exceed  $10 \text{ cm}^{-1}$  and is less than this value for the overwhelming majority of the vibrations.

At the same time, as seen from Fig. 3, the width of the apparatus function of the employed spectral instrument, in the frequency range  $300\text{--}1200 \text{ cm}^{-1}$ , changes from  $5$  to  $30 \text{ cm}^{-1}$ . Consequently, the expected shifts and resonant splittings are beyond the accuracy limits of the experiments for most internal modes. One can therefore expect the treatment of the internal mode in the rigid-lattice approximation to serve as a sufficiently good quantitative basis for the description of the neutron-scattering spectrum in the region  $300\text{--}1300 \text{ cm}^{-1}$ .

The external modes, as shown in<sup>[20]</sup>, are shifted towards the low-frequency side on going from the rigid- to the vibrating-molecule model. The shift is on the average 10% of the phonon frequency. Thus, neglect of the intramolecular motion can lead to an average 10% error in the analysis of the external modes. Since we did not know beforehand the error due to the application of the direct spectral problem to the experi-

TABLE 1. Frequencies (in  $\text{cm}^{-1}$ ) of the internal phonon modes of a naphthalene crystal in the region  $170\text{--}1300\text{ cm}^{-1}$ .

Symmetry type	$\omega_j$	$\omega_j$ Calculation*	$ A_j ^2 \cdot 10^3$ Calculation*	Symmetry type	$\omega_j$	$\omega_j$ Calculation*	$ A_j ^2 \cdot 10^3$ Calculation*
$a_g$	514	476	2.442	$a_u$	212	233	14.719
	763	735	2.786		620	599	5.648
	1022	997	5.647		845	849	12.976
	1148	1148	10.372		975	975	11.894
$b_{1g}$	390	338	9.920	$b_{1u}$	362	349	8.287
	725	729	17.610		820	791	1.871
	933	937	11.954		1126	1107	7.971
	467	440	6.749		1274	1247	6.754
$b_{2g}$	786	824	9.694	$b_{2u}$	618	622	1.654
	878	885	6.516		1008	1004	4.372
	980	1009	9.564		1135	1162	1.242
	509	473	2.333		1212	1220	5.144
$b_{3g}$	936	908	1.921	$b_{3u}$	493	483	15.872
	1468	1124	9.703		480	508	11.732
	1240	1234	7.257		780	803	12.232
					960	967	10.663

Note.  $|A_j|^2 = \sum_{H=1}^8 |A_j^H|^2$ , where  $A_j^H$  is the displacement of the hydrogen atom in a molecule in the  $j$ -th, expressed in units of the amplitudes of the zero-point normal vibrations.

\*Calculation by A. A. Ivlev and M. Ya. Kondratova (private communication).

ment in question, we deemed it possible to base the first comparison of the calculation with experiment on the rigid-molecule approximation.

The simplification of the dynamic problem made it possible to realize the successive cycle of calculations needed for the direct spectral problem.

#### 4. INTERNAL MODES OF THE NAPHTHALENE CRYSTAL

If intermolecular interaction is neglected, the problem of the 96 internal modes reduces to the problem of 48 modes of the free molecule. In this case, the cross section for the single-phonon scattering takes the form

$$\sigma^{\text{inc}}(E_0, E, \varphi, T) = \sum_i \frac{d^2 \sigma_i^{\text{inc}}}{d\omega d\Omega} \quad (5)$$

$$= \frac{k}{k_0} \frac{\hbar |Q|^2}{2\omega} \sum_{i=1}^8 \sum_{j=1}^{48} \frac{(b_i^{\text{inc}})^2}{M_i} |A_j|^2 \delta(\omega - \omega_j) \frac{\exp(-2W_i)}{1 - \exp(-\hbar\omega/kT)}$$

Thus, the spectrum of the single-phonon scattering is a set of 48 functions weighted on the squares of the displacements of the hydrogen atoms<sup>[4]</sup> in each of the vibrations.

The expected experimental scattering spectrum was calculated in accordance with (1) using the scattering cross section in the form (5). The eigenvalues of the vibrational frequencies were taken from the low-temperature spectra of the IR absorption<sup>[25]</sup> and the Raman scattering<sup>[26, 27]</sup> of the crystal. The atom-displacement vectors for each of these vibrations were kindly supplied by A. A. Ivlev as a result of his solution, by a standard calculation method<sup>[28]</sup> of the dynamic problem of the vibrations of a free molecule. The frequency values obtained in this calculation differed somewhat from the experimental ones. These differences, however, did not exceed the values within which, as shown earlier,<sup>[29, 21]</sup> changes of the displacement vectors of the atoms can be neglected. The values of  $\omega_j$  and  $|A_j|^2$  used in the calculations are listed in Table 1.

Figure 4 shows the IINS spectrum and the calculated

single-phonon scattering spectrum. Both spectra are summed over the five angles indicated in the text above. For the comparison with the calculated spectra, we selected the IINS spectrum at  $80^\circ\text{K}$ , the structure of which is still not strongly influenced by the temperature, and whose statistical reliability is approximately double that of the spectrum at  $4.7^\circ\text{K}$ .

As seen from the figure, the calculated scattering spectrum agrees well with the structural part of the experimental spectrum with respect to the positions and widths of the individual bands. If it is assumed that the intensity distributions of the individual bands should be the same as in the calculated spectrum, then it follows that the structural part of the experimental spectrum lies on a continuous structureless background with a maximum in the region from the 40th to the 50th channel, and falling off from the maximum on both sides with different slopes. The stretching of the spectrum is particularly pronounced at lower values of the energy. The shape of the background recalls the spectral distribution with respect to the energies of the incident neutrons and is observed in those cases when the background is due predominately to multiple scattering in the sample. However, since the energies of the incident neutrons are high in the considered region, multiphonon scattering processes are also possible here and can make an additional contribution to the structureless background.

The existence of a background due to multiphonon scattering can be confirmed by an analysis of the spectra shown in Figs. 2b and 2c. The IINS spectra shown in these figures were obtained under identical experi-

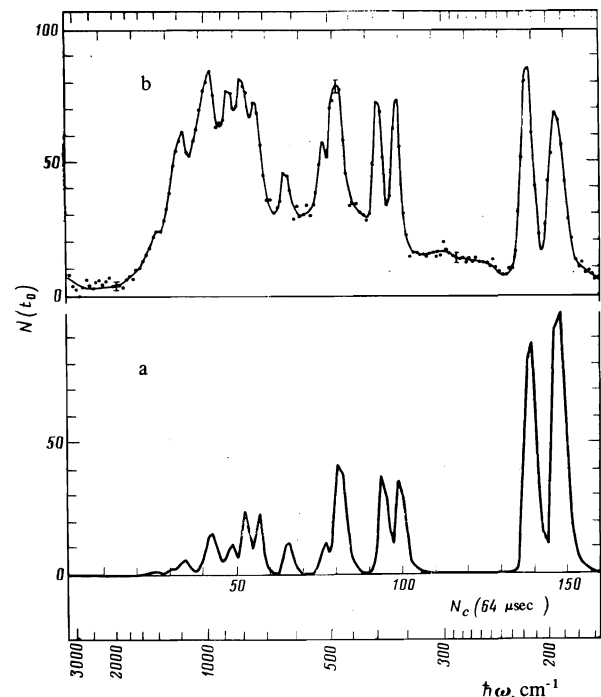


FIG. 4. IINS spectra from the naphthalene crystal in the energy-transfer region  $170\text{--}1300\text{ cm}^{-1}$ : a) calculated single-phonon scattering spectrum,  $T = 83^\circ\text{K}$ ; b) experiment at the same temperature.

mental conditions for a sample placed in an empty cryostat or else in one filled with liquid nitrogen. The measurement time was also practically the same. Under the experimental conditions, the multiple scattering should be the same. Therefore the observed significant change of the spectra can be due only to the multiphonon processes that depend on the temperature. The temperature changes were precisely those expected from different considerations of the multiphonon-scattering spectra.<sup>[8]</sup> The fraction of the multiphonon (apparently mostly two- and three-phonon) in the spectrum at 296 °K becomes larger than the fraction of the single-phonon, and this explains the smoothing out of the structure of the spectra.

The structure of the single-phonon scattering is most clearly pronounced at  $T = 4.7$  °K (Fig. 2a). The abrupt decrease of the background in this spectrum in the channel 60–150 region, in comparison with the spectrum at 296 °K, can be regarded as proof that at 296 °K the background in this region is connected with multiphonon processes. At the same time, its relatively small decrease in the region of channels 30–60 at 4.7 °K in comparison with 296 °K can indicate that this background is the result of multiple scattering. The structure of the IINS spectrum at  $T = 80$  °K (Fig. 2b) is practically similar to the structure of the spectrum at  $T = 4.7$  °K. It is possible that the small differences in the distribution of the intensities of the peaks at channels 94 and 99 are due to the insufficient statistics of the measurements at  $T = 4.7$  °K.

The good agreement between the calculated spectrum of the single-phonon scattering and the observed IINS spectrum shown in Fig. 4 made it possible to draw a large number of conclusions on the structure of the internal modes of the crystal. The agreement between the positions of the maxima of the bands in the experimental and calculated spectra is a reflection of the fact that the values of the frequencies  $\omega_j$ , listed in Table 1 are reliable enough. The bulk of this set constitutes data obtained by optical measurements. However, for a number of vibrations (the separated frequencies in Table 1) the optical data either do not exist at present (symmetry-forbidden  $a_u$  modes), or are not sufficiently reliable. These frequencies were obtained in the present paper by searching for a best fit of the experimental IINS spectra for the calculated ones.

The observed general agreement in the intensity distribution of the IINS spectra in Fig. 4 indicates that the calculated displacements of the atoms of free molecule, listed in Table 1, provide a good quantitative description of the dynamics of the internal phonon modes of the crystal. This means that the molecule force field used in the calculations of A. A. Ivlev, as well as the vibration wave forms obtained by him, can be used to describe the vibrations of the atoms in the crystal.

A comparison of the band widths with the experimental and calculated IINS spectra can also be used to obtain new information. If the scattering spectrum  $\sigma(E_0, E, \varphi, T)$  is represented by a set of  $\delta$  functions, then the width of the individual bands in the calculated spectrum

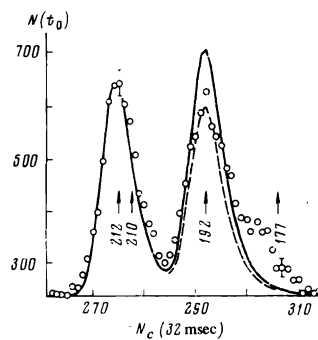


FIG. 5. IINS spectrum from the naphthalene crystal with improved resolution in the region of two low-frequency internal modes,  $T = 80$  °K. Solid and dashed lines—calculation. Points—experiment.

$N(t_0)$  is governed only by the apparatus function (see Fig. 3). In this case the agreement between the widths and positions of the bands of the experimental and calculated spectra is proof of a correct approximation of the apparatus function. The choice of  $\sigma^{\text{inc}}$  in the form (5) for the naphthalene crystal is experimentally justified, inasmuch as the observed values of the factor-group splitting for most modes turn out to be less than the energy widths of the individual channels.

An exception from the general agreement is the band with  $\omega_j = 193$   $\text{cm}^{-1}$  (channel 147), corresponding to the  $b_{3u}$  mode of the free molecule with  $\omega = 176$   $\text{cm}^{-1}$ . The width of the band turns out to be larger in the experimental spectrum than in the calculated one. This suggests that this mode has a noticeable dispersion in the crystal and should therefore have a noticeable factor-group splitting. Indeed, A. Shirokov<sup>[5]</sup> observed in the IR absorption spectrum at 77 °K a doublet of sharply polarized bands with  $\omega = 177$   $\text{cm}^{-1}$  and  $\omega = 192$   $\text{cm}^{-1}$ , which were tentatively combined by him into a Davydov doublet.

To reveal the dispersion more clearly, an additional experiment was performed with somewhat improved resolution.<sup>[6]</sup> Figure 5 shows a section of the IINS spectrum in the region of the two lowest internal molecular modes. The solid line is the calculated IINS spectrum in this region under the assumption that  $\sigma^{\text{inc}}$  is a  $\delta$  function for both modes and the  $\omega_j$  correspond to the data listed in Table 1 at  $T = 80$  °K. The results of the experimental measurements<sup>[7]</sup> at  $T = 80$  °K (sum over five angles) are shown by the points. The vertical bars correspond to the measurement errors.

For a quantitative comparison of the calculated and experimental spectra, the maxima of these spectra were collocated for the mode with  $\omega_j = 212$   $\text{cm}^{-1}$ . As seen from the figure, under these conditions the calculated and experimental band contours of the mode  $\omega_j = 212$   $\text{cm}^{-1}$  coincide with good accuracy within the limits of the experimental error, so that the possible dispersion of this mode does not exceed 3–5  $\text{cm}^{-1}$ . On the other hand, noticeable discrepancies are observed in the region of the mode with  $\omega_j = 193$   $\text{cm}^{-1}$ . The experimental band has a clearly pronounced wing in the region of low energies, and its width in this region is noticeably larger than the calculated value. The auxiliary dashed

TABLE 2. Positions of the maxima of the bands of two low-frequency internal modes in the IINS spectrum

Mode	$\omega_j$	4.7 K	80 K	296 K
$b_{3u}$	193	193.2±0.9	192.7±0.7	187±1
$a_u$	212	216±1	214.7±0.8	208.2±2

curve in Fig. 5, plotted in a scale such that the maxima of the experimental and calculated bands with  $\omega_j = 193 \text{ cm}^{-1}$  coincide, shows that the half-width of the experimental band is also 1.3 times larger than the calculated value. The maximum amplitude of the experimental bands is lower than the calculated value. However, the integrated intensities of both bands, set equal to their areas, turned out to be the same. It follows therefore that the actual density of states in the phonon mode differs from a  $\delta$  function. The summary intensity of the spectrum, as expected, remains as before to  $|a_j|^2$ .

The vertical arrows in Fig. 5 indicate the positions of the components of the factor-group splitting of both modes observed by A. Shirokov in the IR-absorption spectrum of the crystal at 77 °K. For both modes, the Davydov doublets of the bands lie within the limits of the experimental spectra. The values of the Davydov splittings correlate well with the widths of the dispersion regions of the considered phonon modes, determined from the IINS spectra and amounting to  $3 \text{ cm}^{-1}$  for the mode with  $\omega_j = 212 \text{ cm}^{-1}$  and  $17 \text{ cm}^{-1}$  for the mode with  $\omega_j = 193 \text{ cm}^{-1}$ .

The effect of the intermolecular interaction for these modes leads not only to their dispersion and to a factor-group splitting, but manifests itself also in the temperature shifts of the bands of IINS spectrum. Table II shows a change in the positions of the maxima of these bands in the IINS spectrum with changing temperatures. This change takes place simultaneously with the temperature change of the position of the spectrum of the external phonons of the crystal (see Fig. 2).

The pressure of the dispersion and of the temperature shift shows that the rigid-lattice approximation used above for the analysis of the internal modes of the naphthalene crystal is quite rough for the considered two modes, so that a quantitative discussion of these modes calls for the solution of the dynamic problem for them together with the external modes of the crystal.

## 5. EXTERNAL PHONON MODES OF CRYSTAL

In the calculation of the spectrum of the external modes in the rigid-molecule approximation, the force field of the crystal is determined only by the intermolecular-interaction potential. For aromatic crystals, a phenomenological potential for such an interaction was proposed long ago.<sup>[31]</sup> It combines the approximation of the atom-atom interaction<sup>[32]</sup> and the general form proposed by Buckingham for the potential of the paired molecular interaction.<sup>[31]</sup> The potential is given by

$$V(r) = \sum_{i,k} V_{ik}(r) = \sum_{ik} \left[ -\frac{A_n}{r_{ik}^6} + B_n \exp(-\alpha_n r_{ik}) \right], \quad (6)$$

where  $r_{ik}$  is the distance between the  $i$ -th atom of one molecule and the  $k$ -th atom of the other. The parameters  $A_n$ ,  $B_n$ , and  $\alpha_n$  depend only on the sort of the atom. There exist several sets of these parameters for C-C, C-H, and H-H interactions,<sup>[33-35]</sup> and make it possible, accurate to 10-15%, to describe the crystal structure, the thermodynamic functions, and in a number of cases also the spectrum of the limiting frequencies of the external phonons of aromatic crystals.

Our calculations for the naphthalene crystals and the calculations for the benzene crystal<sup>[22]</sup> have shown that the set of the William's parameters<sup>[35]</sup> gives the best agreement between the calculated and experimental data as compared with other sets. The values of the parameters are listed in Table 3.

The frequency spectrum of the naphthalene crystal was calculated in accordance with the formulation of the dynamic problem of the molecular crystal in the atom-atom interaction approximation proposed by Pawley.<sup>[24,36]</sup> We used for the calculation a computer program developed by Pawley. The spectrum was calculated in the harmonic approximation. What were actually observed, however, were noticeable temperature shifts of the limiting frequencies of the external phonon branches<sup>[26]</sup> and a change of the entire spectrum of the external modes (see Fig. 2), which may indicate the presence of anharmonicity. The temperature dependence of the frequencies includes the effect of the change of the volume of the crystal and the purely anharmonic shift. The former effect, also due to anharmonicity, can be taken into account when solving the dynamic problem in the quasi-harmonic approximation. Then the dynamic calculation itself is carried out in the harmonic approximation, and the anharmonicity is introduced phenomenologically via the dependence of the crystal structure data on the temperature. The second effect calls for a special analysis.

The question of the degree to which the temperature shift of the external phonon branches is connected with the change of the volume was solved recently by comparing two series of data on the Raman scattering of the naphthalene crystal.<sup>[37,38]</sup> The first series of data was the result of temperature investigations of the limiting frequencies of the external phonon branches at atmospheric pressure. The second series of data was obtained at room temperature with variation of the pressure. The comparison led to the conclusion that the temperature shift of the frequencies is due practically entirely to a change in volume, and the pure anharmonic effect itself is negligibly small in them. Thus, the use of the quasi-harmonic approximation for the naphthalene

TABLE 3. Values of the parameters of the intermolecular-interaction potential.<sup>[34]</sup>

Type of interaction	A, (kcal/mol)·Å <sup>6</sup>	B, kcal/mole	$\alpha, \text{Å}^{-1}$
C-C	568	83 630	3.60
C-H	125	8766	3.67
H-H	27.3	2654	3.74

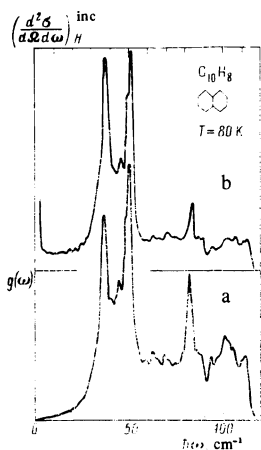


FIG. 6. a) Calculated density of phonon states of the naphthalene crystal  $g(\omega)$ ; b) calculated cross section of single-phonon scattering. The structure data were determined at 120 °K, the limiting radius of the atom-atom interaction was 5.5 Å; scattering at 80 °K.

crystal is justified.

It is natural to assume that the use of the quasi-harmonic approximation is more justified at low temperatures. At the same time, as shown above, the influence of the multi-phonon processes decreases strongly with decreasing temperature. The conditions for comparing the experimental and the calculated data are thus most favorable at low temperatures. We encounter here, however, a difficulty due to the absence of structure data for the naphthalene crystal at low temperatures. The most reliable low-temperature data are known only for 120 °K.<sup>[39]</sup> We therefore used these data in the calculations, and chose for comparison of calculation with experiment the IINS at 80 °K.

Figure 6a shows a histogram of the density of the phonon states of the naphthalene crystal, calculated for 2000 points, using the structure parameters at 120 °K. The interaction radius was 5.5 Å. The single-phonon scattering cross section calculated in accordance with (2) and (3) ( $T = 80$  °K) is shown for the same structure data in Fig. 6b. Although it does reflect the main features of the structures of the density of states, it differs nevertheless noticeably from the latter in the distribution of the intensity at high energies. Figure 7 shows the experimental IINS spectrum in this region and the single-phonon scattering spectrum calculated by using the data of Fig. 6 and expression (1). As seen from the figure, the agreement of the calculated and measured spectra is very good if it is recognized that the disparity between the two principal maxima does not exceed 5  $\text{cm}^{-1}$  in the energy scale, which is close to the accuracy of the optical experiment (the scatter in the experimental values of the limiting frequencies of the phonons in this region is of the same order).

The comparison of the spectra shows convincingly that in the region of the external phonons the inelastic scattering of the neutrons is mainly a single-phonon process. As to the disparity between the positions of the maxima, even though the discrepancy is small in absolute magnitude, it exceeds the resolution of the neutron experiment in this region. The latter circumstances forces us to seek the physical cause of this disparity.

One of the causes may be the fact that the anharmoni-

city was still incompletely accounted for in the calculations, since the employed structure data pertained to a higher temperature than the scattering experiment. The additional decrease of the volume of the crystal cooled to 80 °K leads to a high-frequency shift of the calculated spectrum. It should be noted that allowance for the corrections necessitated by the transition from the rigid-molecule approximation used in the calculation to the complete dynamic problem increases even more the difference between the experimental and calculated spectra, since allowance for the molecule vibrations leads, as follows from<sup>[20]</sup>, to a low-frequency shift.

The observed disparity can be connected also with the choice of the parameters of the potential function (6). Our calculations have shown that the scattering spectrum, at the available resolution level, turns out to be sensitive to the set of parameters  $A$ ,  $B$ , and  $\alpha$ . It can be assumed that if noticeable differences between the experimental and calculated spectra still remain after account is taken of the temperature changes in the structure, then these differences can be used to improve the dynamic model of the crystal, to change over to higher approximation of the dynamic problem in comparison with the ones used in the present paper, and to improve the parameters of the potential.

## CONCLUSION

It follows from the foregoing data that the approach based on a consistent solution of the direct spectral problem and on the comparison of the results with the experimental spectrum is effective. This approach leads to sufficiently reliable conclusions concerning the character of the neutron scattering relative to the one- and multiphonon excitations, concerning the validity of the models of the dynamic system of the crystal used to describe its phonon spectrum. Thus, an analysis of the obtained experimental and calculated data on the naphthalene crystal has demonstrated the following.

1. The rigid-lattice model, which is the basis of the

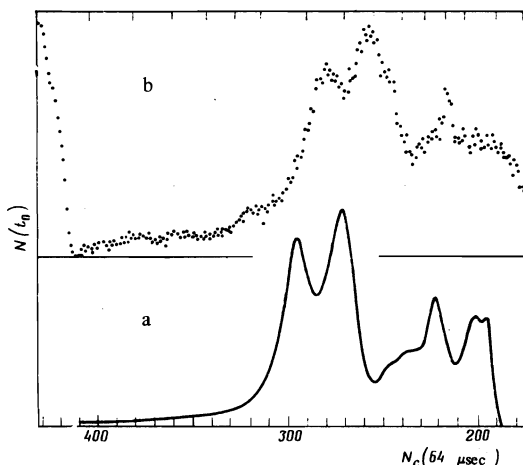


FIG. 7. IINS spectra of naphthalene crystal in the energy-transfer region 0-140  $\text{cm}^{-1}$ ; a) calculated single-phonon scattering spectrum; b) experiment,  $T = 80$  °K.



quantitative description of the internal phonon modes of the spectrum of the naphthalene crystal, was convincingly confirmed experimentally for 29 modes in the energy range 170–1300  $\text{cm}^{-1}$ . From the general agreement between the distribution of the intensity of the structure peaks on Fig. 4 follows an experimental proof of the validity of the quantitative description, obtained within the framework of this model, of the wave form and the frequencies of the majority of the internal vibrations of the naphthalene molecule in the crystal. Only one mode (at  $\omega_j = 183 \text{ cm}^{-1}$ ) revealed a noticeable dispersion, so that the extension of the dynamic model with allowance for the intermolecular interactions should concern this mode. The density of the phonon states in this region of the spectrum is well described by a set of 28  $\delta$  functions. The dispersion of the 183 and 212  $\text{cm}^{-1}$  mode is respectively  $\sim 17$  and  $3 \text{ cm}^{-1}$ .

2. In the region of the external phonon modes, a sufficiently good agreement is observed between the calculated and experimental data for  $T = 80^\circ \text{K}$ . This leads, first, to an important practical conclusion that the spectrum of the crystal frequencies shown in Fig. 6b is a sufficiently good representation of the true spectrum, and therefore can be used subsequently, with small corrections, for both a quantitative investigation of the thermodynamic characteristics of a crystal, and to construct the models of the electron and vibron-phonon interactions in the optical spectra of naphthalene at low temperatures.

The authors are deeply grateful to Dr. S. Pawley for making available the computer program for the solution of the problem of the external phonons of the naphthalene crystal, to L. A. Gribov and A. A. Ivlev for supplying the data on the calculation of the vibration frequencies and the displacement vectors of the atoms in the naphthalene molecule, to L. O. Atovmyan, V. I. Ponomarev, and O. S. Filippenko for performing at our request low-temperature measurement of the structure of the naphthalene crystal, to E. M. Rodina for developing the computer programs for the scattering cross sections and for the direct spectral problem, and for performing the calculations, to V. L. Broude and E. A. Yanik for a discussion of the results, and to S. I. Bragin, V. P. Zhebelev, and Ja. Domoslawski for help with the experiments.

<sup>1</sup>Nuclear Physics Institute, Krakow, Poland.

<sup>2</sup>The function  $A(E_0, E, t_0, t) = \delta(t_0 - t - \alpha L_1/\sqrt{E_0} - \alpha L_2/\sqrt{E})$  represents the condition for registering, at the instant of time  $t_0$ , a neutron emitted from the source at the instant  $t$  with energy  $E_0$  and scattered by the sample to an energy  $E$ .

<sup>3</sup>See the diploma thesis of A. V. Sermyagin, Nuclear Physics Laboratory, JINR, 1972.

<sup>4</sup>Owing to the anomalously large amplitude of the incoherent scattering and the small mass of the hydrogen atom, neutron scattering by hydrogen-containing compounds can be described with high accuracy by scattering from hydrogen atoms.<sup>[30]</sup>

<sup>5</sup>See the diploma thesis of A. Shirokov, Institute of Solid State Physics, 1972.

<sup>6</sup>The resolution was improved by reducing to one-half the width of the transmission band of the monochromator crystal (zinc single crystal), superposing on its absorption edge a beryllium filter. The improvement in the resolution was 30%.

<sup>7</sup>The experimental conditions were the same as those used to obtain the spectrum at  $80^\circ \text{K}$ , shown in Fig. 4. The measurement time was 100 hours.

<sup>1</sup>G. Placzek and L. van Hove, Phys. Rev. **93**, 1207 (1954).

<sup>2</sup>Yu. Kagan, Zh. Eksp. Teor. Fiz. **40**, 312 (1961) [Sov. Phys. JETP **13**, 211 (1961)].

<sup>3</sup>Yu. Kagan, *ibid.* **42**, 1375 (1962) [15, 954 (1962)].

<sup>4</sup>V. F. Turchin, Medlennye neitrony (Slow Neutrons), Atomizdat, 1963.

<sup>5</sup>W. Marshall and S. W. Lovesey, Theory of thermal neutron scattering, Oxford, Clarendon Press, 1971.

<sup>6</sup>I. P. Ereemeev, I. P. Sadikov, and A. A. Chernyshov, Preprint IAE-2228, 1972.

<sup>7</sup>I. P. Ereemeev, I. P. Sadikov, and A. A. Chernyshov, Fiz. Tverd. Tela **15**, 1953 (1973) [Sov. Phys. Solid State **15**, 1309 (1974)].

<sup>8</sup>I. I. Gurevich and A. V. Tarasov, Fizika neitronov nizkikh energii (Physics of Low Energy Neutrons), Nauka, 1965.

<sup>9</sup>K. Parlinski, M. Sudnik-Hryniewicz, A. Bajorek, J. A. Janik, and W. Olearczyk, in: Research applications of nuclear pulsed systems, IAEA, Vienna, 1967, p. 179.

<sup>10</sup>M. Mendes and C. de Polignac, Acta Crystallogr. **A29**, 1 (1973).

<sup>11</sup>A. N. Tikhonov and V. Ya. Arsenin, Metody resheniya nekorrektnykh zadach (Methods of Solving Incorrect Problems), Nauka, 1974.

<sup>12</sup>G. S. Pawley, P. A. Reynolds, J. K. Kjems, and J. W. White, Solid State Commun. **9**, 1353 (1971).

<sup>13</sup>G. H. Vineyard, Phys. Rev. **96**, 93 (1954).

<sup>14</sup>H. Eschrig, L. van Loyen, and P. Ziesche, Phys. Status Solidi **66b**, 587 (1974).

<sup>15</sup>W. Drexel and I. Natkaniec, Ann. Rep. ILL, Grenoble, 0401020, 1973.

<sup>16</sup>K. W. Logan, S. F. Trevino, H. J. Prask, and J. D. Gault, J. Chem. Phys. **53**, 3417 (1970).

<sup>17</sup>A. Bajorek, T. A. Machekhina, K. Parlinski, and F. L. Shapiro, in: Inelastic scattering of neutrons, VII, IAEA, Vienna, 1965, p. 519.

<sup>18</sup>I. M. Frank, Fiz. Elem. Chastits At. Yadra **2**, No. 4, 1 (1972) [Sov. J. Part. Nucl. **2**, 805 (1973)].

<sup>19</sup>H. Eschrig, K. Feldman, K. Henning, W. John, and L. van Loyen, Phys. Status Solidi **58b**, K159 (1973).

<sup>20</sup>G. S. Pawley and S. J. Syvin, J. Chem. Phys. **52**, 4073 (1970).

<sup>21</sup>G. Taddei, N. Bonadeo, M. P. Marzocchi, and S. Califano, J. Chem. Phys. **58**, 966 (1973).

<sup>22</sup>G. Vankataraman and V. C. Sahni, Rev. Mod. Phys. **42**, 409 (1970).

<sup>23</sup>G. Taddei and S. Califano, Rivista Nuovo Cimento **1**, ser. I, 547 (1969).

<sup>24</sup>G. S. Pawley, Phys. Status Solidi **20**, 347 (1967).

<sup>25</sup>K. Tsuji and H. Yamada, J. Phys. Chem. **76**, 260 (1972).

<sup>26</sup>M. Suzuki, T. Yokoyama, and M. Ito, Spektr. Acta **24A**, 1091 (1968).

<sup>27</sup>D. M. Hanson and A. R. Gee, J. Chem. Phys. **51**, 5052 (1969).

<sup>28</sup>V. A. Dement'ev, O. I. Kondratov, L. A. Gribov, and L. I. Kashkan, Izv. Timir. s/khoz. akad. **2**, 203 (1970).

<sup>29</sup>G. Hagen and S. J. Syvin, J. Phys. Chem. **72**, 1446, 1451 (1968).

<sup>30</sup>J. W. White, Molecular Spectroscopy, 1966, p. 215.

<sup>31</sup>R. A. Buckingham, Proc. R. Soc. Lond. **A168**, 264 (1938); J. Corner, Proc. R. Soc. Lond. **A189**, 118 (1947).

<sup>32</sup>A. I. Kitaigorodski, J. Chim. Phys. Physicochim. Biol. **63**, 9 (1966).

<sup>33</sup>A. I. Kitaigorodskii and K. V. Mirskaya, Kristallografiya **6**, 507 (1961); **9**, 174 (1964) [Sov. Phys. Crystallogr. **6**, 408 (1962); **9**, 137 (1964)].

<sup>34</sup>D. E. Williams, J. Chem. Phys. **45**, 37710 (1966); **47**, 4680 (1967).

<sup>35</sup>K. V. Mirskaya, I. E. Kozlova, and V. F. Bereznitskaya, Phys. Status Solidi 62b, 291 (1974).

<sup>36</sup>G. S. Pawley, Phys. Status Solidi 49, 475 (1972).

<sup>37</sup>D. A. Dows, L. Hsu, S. S. Mitra, O. Brafman, M. Hayek, W. Daniels, and R. K. Crawford, Chem. Phys. Lett. 22, 595 (1973).

<sup>38</sup>O. Brafman, Chem. Phys. Lett. 24, 381 (1974).

<sup>39</sup>V. I. Ponomarev, O. S. Filippenko, and L. O. Atovmyan, Kristallografiya 21, 392 (1976) [Sov. Phys. Crystallogr. 21, 215 (1976)].

Translated by J. G. Adashko

## Impedance of superconducting tin in a magnetic field at frequencies of 300–1200 MHz

S. A. Govorkov and V. A. Tulin

*Institute of Solid State Physics, Academy of Sciences of the USSR, Chernogolovka*

(Submitted August 22, 1975)

Zh. Eksp. Teor. Fiz. 70, 1044–1050 (March 1976)

An investigation was made of the active component of the impedance of superconducting tin at frequencies 300–1200 MHz in magnetic fields below the critical value. The field dependence of this component had an absorption maximum at  $H=0$  throughout the investigated frequency range. The amplitude of the absorption maximum decreased rapidly when temperature was reduced below the critical value. The temperature dependence was anisotropic and the width of the absorption peak changed considerably when the frequency was increased. The results were analyzed on the basis of surface levels formed by normal excitations in a superconductor subjected to a magnetic field.

PACS numbers: 74.20.Gh, 74.50.Gz

### INTRODUCTION

Electrons in metals may be reflected specularly from a sufficiently smooth metal–vacuum boundary and in the presence of a magnetic field they may form bound surface states known as magnetic surface levels. At microwave frequencies these bound electrons make a considerable contribution to the surface current and are responsible for the easily observed resonance spectra of magnetic surface levels.<sup>[1,2]</sup> In the rf range some of the levels are not resolved and their spectrum is quasi-continuous; in this case the contribution of surface electrons to the impedance is a peak in zero magnetic field.<sup>[3]</sup> In the superconducting state of metals there are normal electrons, which exist for  $T \neq 0$ , that can also form surface states in the presence of a magnetic field, as observed by Maldonado and Koch at frequencies of 10–70 GHz.<sup>[4]</sup> In the rf frequency range it is not possible to observe the contribution of normal electrons to the impedance because of the screening action of the superconducting condensate. When the frequency is increased, the contribution of normal electrons to the surface impedance increases and at frequencies exceeding  $10^8$  Hz it becomes possible to observe normal carriers.

Investigations of the impedance of superconductors at frequencies used in the present study were carried out by Pippard<sup>[5]</sup> and Spiewak.<sup>[6]</sup> Pippard investigated the temperature dependence of the real part of the surface impedance of tin in zero magnetic field associated with the screening action of the superconducting condensate. Spiewak studied the dependence of the surface impedance on the magnetic field but the shape of the samples and the configuration used in his work were such that it was not easy to isolate the absorption due to surface levels. We used samples prepared from pure tin and the orien-

tation of the surface of a sample relative to static and hf magnetic fields was optimal for the observation of surface levels.

### METHOD AND SAMPLES

We determined the dependence of the derivative  $dR/dH$  of tin on the magnetic field applied at 300–1200 MHz ( $R$  is the real part of the surface impedance and  $H$  is the magnetic field). A block diagram of the apparatus is shown in Fig. 1. The microwave power was generated by an oscillator and passed through a resonator to a measuring receiver. After amplification and phase-sensitive detection the signal was plotted by an X–Y recorder. The resonator was a helix made of electrical-

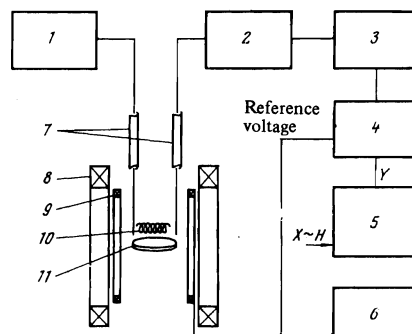


FIG. 1. Block diagram of the apparatus for investigating the dependence of  $dR/dH$  on the magnetic field in the frequency range 300–1200 MHz: 1) oscillator (300–1200 MHz); 2) receiver (200–1200 MHz); 3) amplifier (30 Hz); 4) phase-sensitive detector; 5) X–Y plotter; 6) oscillator (30 Hz); 7) coaxial lines; 8) Helmholtz coils; 9) modulation coils; 10) resonator helix; 11) sample.